

ELECTRONIC SUPPORTING INFORMATION

The role of specific and active surface areas in optimizing hard carbon irreversible capacity loss in sodium ion batteries

Adrian Beda,^{a,b,c} Cyril Vaultot,^{a,b} François Rabuel^{c,d}, Matthieu Morcrette^{c,d} and Camélia Matei Ghimbeu^{a,b,c*}

^a*Université de Haute-Alsace, CNRS, Institut de Science des Matériaux de Mulhouse (IS2M) UMR 7361, F-68100 Mulhouse, France*

^b*Université de Strasbourg, F-67081 Strasbourg, France*

^b*Réseau sur le Stockage Electrochimique de l'Energie (RS2E), HUB de l'Energie, FR CNRS 3459, 80039 Amiens Cedex, France*

^d*Université de Picardie Jules Verne, Laboratoire de Réactivité et Chimie des Solides (LRCS), UMR 7314 CNRS, HUB de l'Energie, 80039 Amiens, France*

Experimental procedure

- **Materials synthesis**

The hard carbon materials synthesis was fully described in our previous work ¹ (HCS series - in the main manuscript and the other materials in the ESI section). Briefly, HCS carbons were obtained by precipitation-polymerization of a phenolic resin (phloroglucinol-glyoxylic acid) at room temperature ^{1,2} in the presence of a cross-linker (triethylenediamine, TEDA) in water. The obtained polymer product was pyrolysed under Ar at temperatures between 1300 and 1600 °C, and the derived carbons were labelled HCST (where T-denotes the pyrolysis temperature). The TCA1300 and TCA1400 materials were synthesized similarly to the HCS; however, thiophene carboxaldehyde (TCA) and L-cysteine were additionally added to the reaction mixture ¹. Pyrolysis was performed at 1300 and 1400 °C. For the synthesis of PR1400 carbon, a polymerization route using phloroglucinol and glyoxylic acid in ethanol was used ^{1,3}, followed by the pyrolysis of the obtained polymer at 1400 °C. HAB1300 and HAB1400 carbons were prepared by hydrothermal carbonization of a solution of glucose at 180 °C, and the obtained hydrochars were pyrolysed at 1300 °C and 1400 °C, respectively¹. PAC2 is a commercial carbon purchased from Aekyung Petrochemical, South Korea.

- **Materials characterisation**

All the physico-chemical analyses were made on hard carbon powders while the electrochemical tests on the carbon electrodes. Worth to mention, that some differences between the properties of powder and of electrode might exist which are not considered herein.

The total surface area (TSA) of hard carbon materials was determined by O₂ adsorption according to our recent findings⁴. The O₂ adsorption/desorption isotherms were recorded at 77 K using an ASAP 2020 instrument (Micromeritics). First, the materials were outgassed overnight under vacuum at 300 °C to remove the water molecules. Additionally, 2 h of outgassing was conducted on the analysis port to remove any gas molecules that could be trapped in the carbon pores. The dead volumes of the analysis

tube were calibrated after the analysis to avoid any gas adsorption in the materials that could occur if this step was performed at the beginning of the analysis (classical procedure). Low pressure incremental O₂ doses were applied, i.e., 5 cm³ g⁻¹ for high surface area materials and between 0.05 and 1.0 cm³ g⁻¹ for low surface area materials. The total surface area was determined using the Brunauer–Emmett–Teller (BET) model from the linear plot of the relative pressure, P/P₀, which had a range of 0.01-0.05. The total pore volume (V_T) was assessed at a relative pressure of P/P₀ = 0.99.

The pore size distribution (PSD) was determined on the O₂ adsorption branch using SAIEUS (Solution of Adsorption Integral Equation Using Splines) software (Micromeritics) ⁵. The two-dimensional nonlocal density functional theory (2D-NLDFT) pore model for carbons with heterogeneous surfaces was selected. The pore average diameter (L₀) was calculated as described elsewhere⁴. The adsorption analyses measurement error is estimated between 5 and 10 %, depending on the material.

The active surface area (ASA) was determined by TPD-MS after oxygen chemisorption on hard carbons ⁶. In the first step, the materials were heat-treated up to 950 °C under secondary vacuum to remove the oxygen-based and other functional groups. Then, the sample was cooled to 300 °C and subjected to O₂ chemisorption for 10 h, followed by TPD-MS analysis to monitor the evolution of CO and CO₂ gases while increasing the temperature. The ASA is calculated considering the amounts of CO and CO₂ evolved and the area of an edge carbon site, according to the following formula:

$$\mathbf{ASA [m^2 g^{-1}] = (n_{CO} + 2n_{CO_2}) \times A \times N_A} \quad (1)$$

Where:

n- number of moles [mol g⁻¹]

A - average area of an edge carbon atom [0.083 nm² = 8.3 · 10⁻²⁰ m²] ⁷

N_A - Avogadro constant [6.022 · 10⁻²³ mol⁻¹]

It is assumed that ⁷: a) each C-O complex has an oxygen atom bonded to an edge carbon, b) the edge carbons lie in the (100) plane and (c) within the graphite structure, each carbon atom occupies an average area of 0.083 nm².

X-ray photoelectron spectroscopy (XPS) was employed to investigate the carbon chemical composition (~ 10 nm surface). A VG Scienta SES-2002 spectrometer equipped with a monochromatic X-ray source (Al K α , 1486.6 eV) operating at 420 W (14 kV; 30 mA) was used.

Raman spectra were acquired with a LabRAM BX40 (Horiba Jobin-Yvon) spectrometer equipped with a He-Ne excitation source (532 nm wavelength). Nine spectra were recorded, and the average spectrum was used to calculate the I_D/I_G ratio.

- **Materials electrochemical characterisation**

The HC electrodes were prepared by mixing the hard carbon with a polyvinylidene fluoride (PVdF) binder and carbon black (SUPER C45, TIMCAL) in a mass ratio of 94:3:3 in the presence of N-methyl-2-pyrrolidone (NMP). The obtained slurry was laid on an Al current collector; disks of 1 cm and a mass loading of 5-10 mg cm⁻² were obtained. Half-cells were assembled using sodium metal as the counter/reference electrode and a glass fibre separator. The electrolyte was 1 M NaPF₆ in a mixture (1:1) of ethylene carbonate (EC)/dimethyl carbonate (DMC). Galvanostatic charge–discharge tests were performed with a VMP3 Bio-Logic setup at a constant current in a voltage window between 0.01 and 2 V (versus Na⁺/Na) at a C/50 rate. The potentials are expressed relative to Na metal (vs. Na⁺/Na). More details about the electrochemical testing procedure can be found elsewhere ¹.

The irreversible capacity loss (ICL) of the first electrochemical cycle was determined by the following formula:

$$ICL (\%) = \frac{C_D - C_C}{C_D} \times 100 \quad (2)$$

where C_D and C_C represent the specific capacity of the first discharge and charge, respectively. The theoretical capacity was 372 mAh g⁻¹.

Results

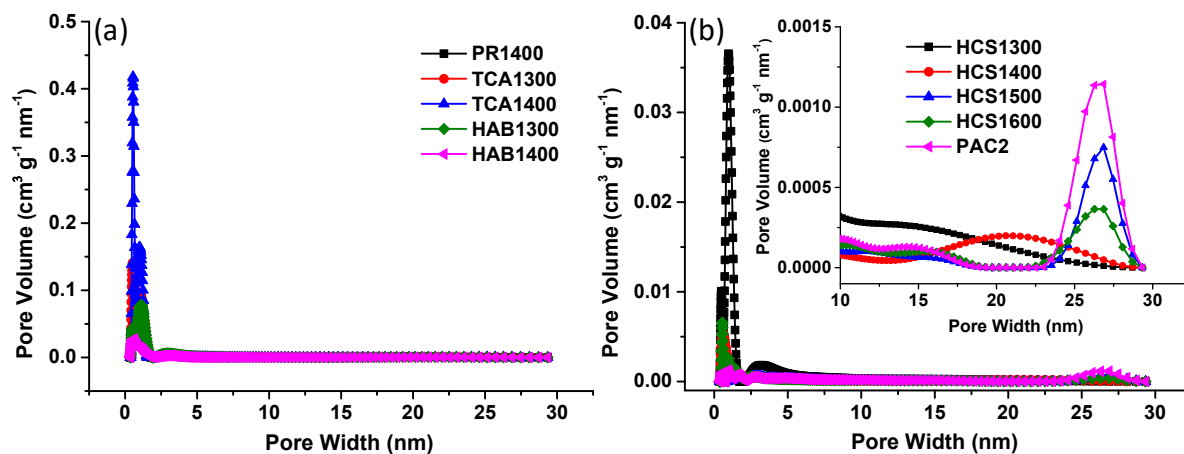


Figure S1: 2D-NLDFT pore size distribution of hard carbon materials in the 0-30 nm range: (a) high surface area and (b) low surface area materials. Inset: zoom on the 10-30 nm pore size range.

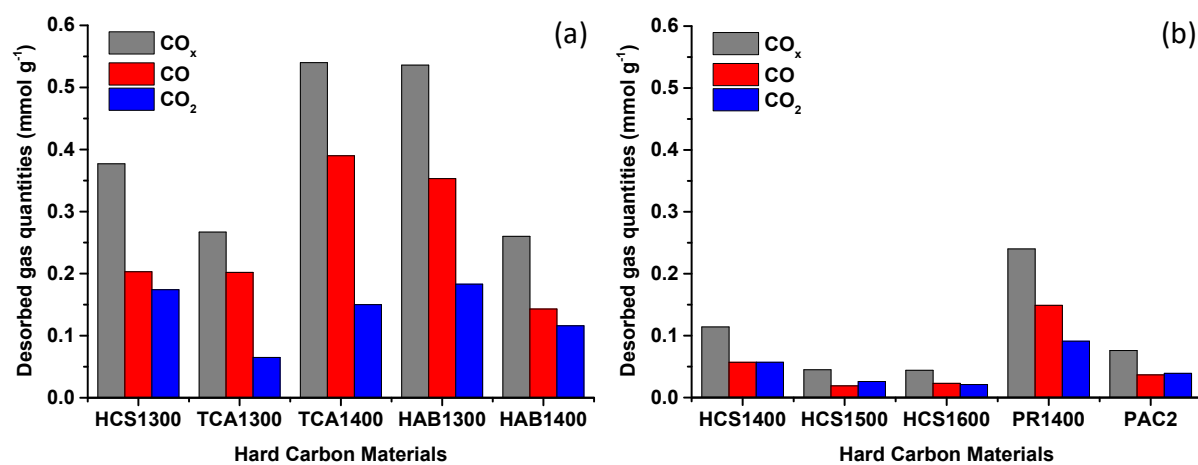


Figure S2: Amounts of desorbed CO, CO₂ and total CO_x groups as determined by TPD-MS after the O₂ chemisorption step.

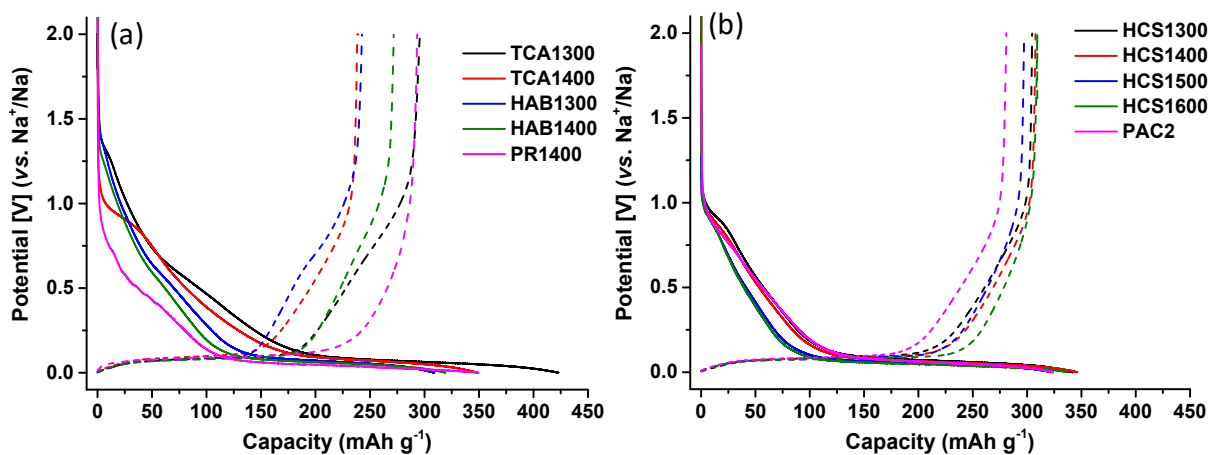


Figure S3: Charge/discharge profiles for the 1st cycle of the cells assembled with different hard carbons and 1 M NaPF₆ in EC:DMC electrolyte: (a) high and (b) lower irreversible capacity materials.

Table S1: XPS chemical composition of selected HCs treated at 1300 °C.

Materials	C at%	O at%	Si* at%	S at%	Csp ² %	Csp ³ %	Ratio O/C
HCS1300	96.11	3.15	0.75	-	88.80	1.68	0.032
TCA1300	97.28	2.22	-	0.50	90.02	1.60	0.022
HAB1300	97.12	2.88	-	-	86.72	3.13	0.029

*- might come from the XPS analysis tape

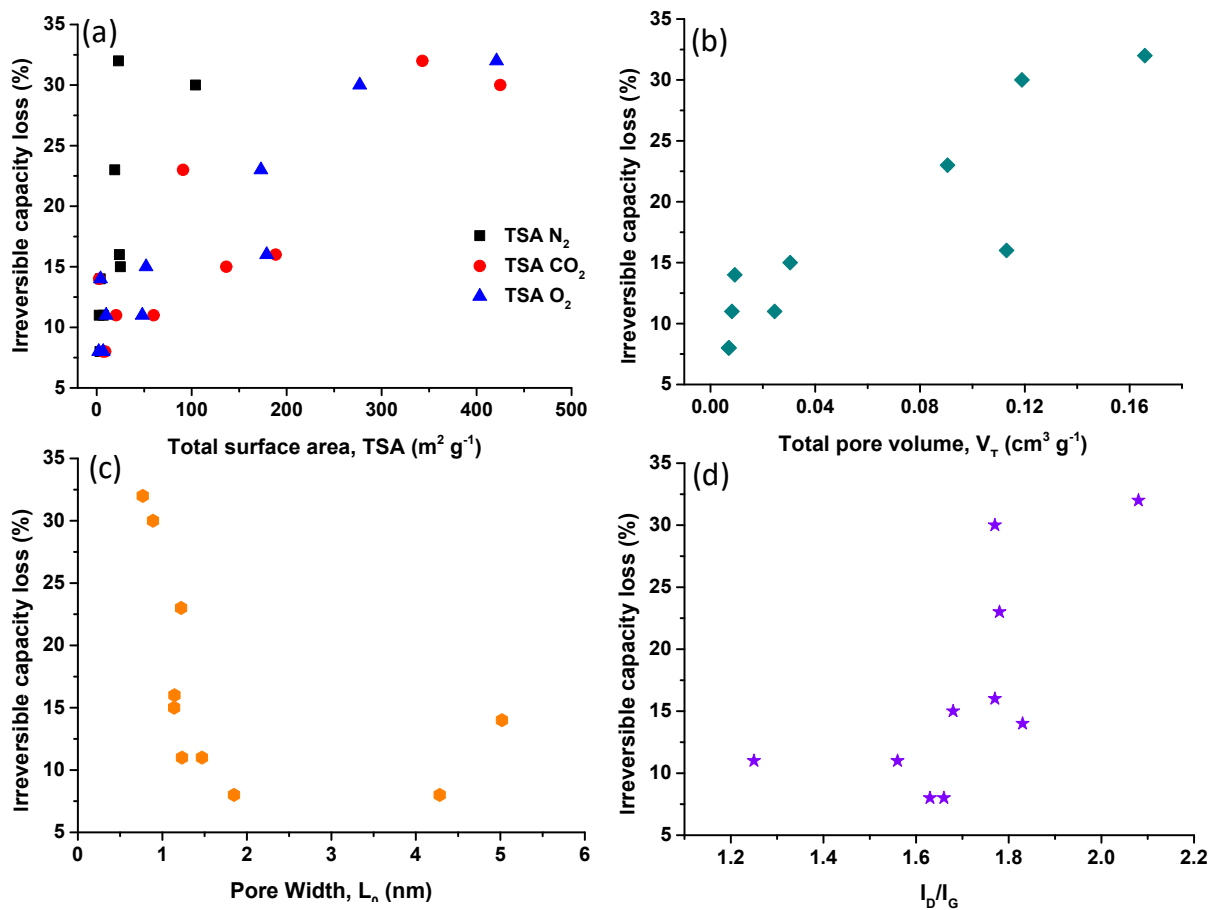


Figure S4: Correlation between the irreversible capacity loss and: (a) total surface area, TSA, determined by N₂, CO₂ and O₂ adsorption, (b) total pore volume, V_T determined by O₂ adsorption and (c) average pore width, L₀ obtained by O₂ adsorption and (d) I_D/I_G Raman ratio. The N₂ and CO₂ total surface areas were extracted from our previous work ¹.

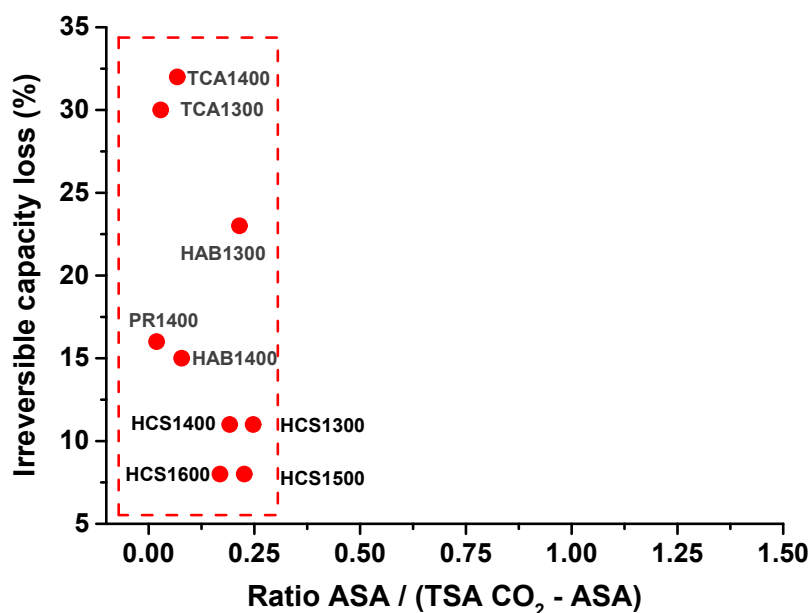


Figure S5: Relationship between the 1st irreversible capacity loss and the ratio ASA/(TSA CO₂-ASA).

References

1. A. Beda, F. Rabuel, M. Morcrette, S. Knopf, P. L. Taberna, P. Simon and C. Matei Ghimbeu, *J Mater Chem A*, 2021, **9**, 1743-1758
2. A. Maetz, L. Delmotte, G. Moussa, J. Dentzer, S. Knopf and C. M. Ghimbeu, *Green Chemistry*, 2017, **19**, 2266-2274.
3. A. Beda, P.-L. Taberna, P. Simon and C. Matei Ghimbeu, *Carbon*, 2018, **139**, 248-257.
4. A. Beda, C. Vaultot and C. M. Ghimbeu, *Journal of Materials Chemistry A*, 2021, **9**, 937-943.
5. J. Jagiello and J. Olivier, *Carbon*, 2013, **55**, 70-80.
6. C. Matei Ghimbeu, J. Górká, V. Simone, L. Simonin, S. Martinet and C. Vix-Guterl, *Nano Energy*, 2018, **44**, 327-335.
7. N. R. Laine, F. J. Vastola and J. P. L. Walker, *J. Phys. Chem*, 1963, **67**, 2030-2034.